Hall Current Plasma Accelerator

GORDON L. CANN* AND GARY L. MARLOTTE†
Electro-Optical Systems, Inc., Pasadena, Calif.

Theoretical and experimental investigations are being carried out on a relatively new type of accelerator, the Hall current plasma accelerator. This paper deals with a self-contained portion of a theoretical investigation and will be followed by other papers dealing with additional theoretical results and experimental results. The particular configuration under study employs the radial component of a fringing magnetic field and the Hall induced current of an axial discharge to obtain the electromagnetic acceleration of a neutral plasma. Using terms derived on the basis of a three-particle gas kinetic theory, a gasdynamic analysis is made using a simplified model of this configuration. Regimes of operation for a constant area accelerator are outlined, showing the importance of the critical parameters of Mach number and ion slip ratio. Integral solutions are obtained showing that arbitrarily high velocity ratios across the accelerator are obtainable. Expressions for the thrust efficiency are obtained and evaluated.

1. Introduction

IN recent years, many new devices have evolved for the electromagnetic acceleration of a neutral plasma. Primary applications have been in the fields of space propulsion and hypervelocity wind tunnels. Recently a new concept for plasma acceleration has been advocated: the Hall current plasma accelerator.[1]

In the system proposed in Ref. 1 and sketched in Fig. 1, an electric field is applied axially to a stream of flowing plasma by a pair of electrodes. An external electromagnet is employed to generate a magnetic field with a strong radial component. When the axial field is applied and a current flows through the plasma, an azimuthal component of current is induced, i.e., the Hall current. The azimuthal current interacting with the radial magnetic field gives rise to an axial Lorentz force, which accelerates the plasma. An alternative field arrangement can be used in which the magnetic field is axial or parallel to the plasma flow, and the applied electric field is radial. A Hall accelerator with this configuration is currently under investigation by Hess et al.[2, 3]

Close relatives to the forementioned Hall accelerators (or electrostatic neutral plasma accelerators) include the magnetic annular arc,[4] the oscillating-electron ion engine,[5] and the cyclotron resonance plasma accelerator.[6]

2. Physical Concepts of Hall Acceleration

There are actually two bases upon which the physical principle of Hall acceleration of a neutral plasma can be explained. One is in terms of $\mathbf{J} \times \mathbf{B}$ or Lorentz forces acting upon a continuum plasma and the other in terms of the acceleration of ions in an electric field. For either, the schematic representation of a Hall accelerator given in Fig. 1 is applicable.

To obtain Hall acceleration, the magnetic field strength is made high and the plasma properties are controlled so that the Larmor radius is small compared to the mean free path for the electrons but is large for the ions; i.e., $\omega_e\tau_e \gg 1$ and $\omega_I\tau_I \ll 1$, in which ω is the cylotron frequency and τ is the mean time between collisions. Under such conditions and when an axial current flows, a Hall component of current flows in the azimuthal or θ direction. The Hall current can be made large compared to the axial current by making $\omega_e\tau_e$ large, of the order of 10 or higher. The azimuthal Hall current interacting with the applied radial magnetic field produces an axial Lorentz force that acts upon and accelerates the plasma. Since the Hall current is large compared to the ordinary or axial current, the axial Lorentz force dominates, thus providing useful acceleration to the plasma. Based on this phenomenon, the name Hall current accelerator was adopted.[1]

Consider now the plasma acceleration from a particle viewpoint. When an axial electric field is applied to the plasma with no magnetic field present, the forces exerted upon the ions and the electrons are identically equal and opposite. Normally, no net momentum is added to the system although the ions and electrons are accelerated in opposite directions. Because of the higher electron mobility, the electrons receive most of the energy. However, when a strong radial magnetic field is applied so that $\omega_e\tau_e \gg 1$, the mobility of the electrons in the axial direction is greatly reduced. Since normally $\omega_I\tau_I$ will remain small, the ion mobility is not appreciably increased. Hence, the electric field energy is now given mainly to the ions instead of to the electrons, and the ions are "electrostatically" accelerated in the direction of the electric field. By collisions the particles are also accelerated. Therefore, the entire neutral plasma is accelerated.

On the basis of these physical concepts, the theoretical description of Hall current acceleration is derived. The two physical descriptions just given will be shown to be mathematically equivalent.

A model of the Hall accelerator will be used which consists of an annulus across which a radial magnetic field is applied. Current will be drawn through the annulus by applying an electric field between electrodes placed at either end of the annulus. In this model, there is no radial force applied to the gas; hence, radial components of mass motion and diffusion are considered to be zero. The magnitude of the induced tangential magnetic field due to the axial current will be assumed to be negligible with respect to that of the applied magnetic field. Thermoelectric potentials are also considered to be negligible. In practice, it is not easy to obtain a long annulus through which a uniform radial magnetic field extends, and some configuration similar to that shown in Fig. 1 needs to be adopted.

Before a gasdynamic analysis can be made, expressions are needed for the momentum and energy exchanged per unit volume between the gas and the magnetic field. These expressions are discussed below (see Refs. 7–9 for their derivations).

There is assumed to be no charge concentration ($n_I = n_e$), and terms of the order of the square root of the electron to

Received October 10, 1963; revision received May 4, 1964. Work described in this paper was performed under Contract NAS3-2500 for the NASA Lewis Research Center.

* Manager, Plasma Physics Department. Member AIAA.
† Research Physicist, Plasma Physics Department. Member AIAA.

ion mass ratio are neglected compared to unity. In addition, the restriction $(1 - \tau) \ll 1$ is made, where τ is the ratio of the ion to electron temperature; in practice, this means that the electrons may have no more than of the order of 25% greater temperature than the heavy particles before neglected terms become important.

2.1 Force Equations

The axial force per unit volume X_z which is applied to the gas is expressed by[7-9]

$$\frac{X_z}{|e|n_I} = \frac{\psi_e^2(E_z - vB) - \psi_e(1 + \psi_e\psi_I)w|B|}{\psi_e^2 + (1 + \psi_I\psi_e)^2} = \frac{\psi_e|B|}{1 + \psi_e\psi_I}\left\{\frac{j_z}{|e|n_I} - w\right\} = -\frac{j_\theta B}{|e|n_I} \quad (1)$$

The tangential force per unit volume X_θ which the gas experiences is given by[7-9]

$$\frac{X_\theta}{|e|n_I} = \frac{\psi_e(1 - \psi_e\psi_I)(E_z - vB)\cdot(B/|B|) + \psi_e^2 wB}{\psi_e^2 + (1 + \psi_I\psi_e)^2} = \frac{j_z B}{|e|n_I} \quad (2)$$

For a discussion of the equations, including an axial magnetic field component, see Ref. 7.

The ratio of the axial to tangential forces can be expressed as

$$\frac{X_\theta}{X_z} = \frac{1 + \psi_e\psi_I}{\psi_e}\frac{B/|B|}{[1 - (|e|n_I w/j_z)]} \quad (3)$$

The parameter ψ_e is equal to the usual $\omega_e\tau_e$, but the parameter ψ_I does not have such a simple physical interpretation. It can be written as

$$\psi_I = \omega_I\tau_I = \omega_I\tau_I'[n_a/(n_a + n_I)]^2$$

Here ω_I is the cyclotron frequency of the ions, and τ_I' is the average collision time for ions and atoms. The square of the ratio of atom density to that of the sum of ion and atom density modifies the quantity $\omega_I\tau_I'$. Similar to $\omega_e\tau_e$ for the electrons, $\omega_I\tau_I'$ can be interpreted as the cycles per collision which the ions undergo. The remaining notation is conventional. These equations, along with the original diffusion equations,[1] show the following:

1) The axial force is symmetric in the magnetic field except for the small term vB, so that reversing the magnetic field has no effect on it. In addition, the axial force depends quadratically on the magnetic field for small magnetic fields, but when $\psi_e\psi_I \gg 1$, the magnitude of the axial force becomes independent of the magnitude of the radial magnetic field.

2) The tangential force is antisymmetric in the magnetic field except for the small term vB, and the tangential currents reverse when the magnetic field is reversed.

3) With reference to a real device, the current components will tend to distribute themselves differently over the radius, with the tangential currents spreading away from regions of high velocity toward the walls and the axial currents concentrating in the central freestream annulus region where the velocity and ion density are the highest.

4) When the magnetic field is strong enough so that $\psi_I\psi_e \gg 1$, then the diffusion equations[7] show that the electron diffusion velocity becomes very closely equal in magnitude, but opposite in direction, to the gas velocity, e.g., the electrons are effectively trapped by the magnetic field and remain stationary in space ($w_e = -w$); this indicates that the current density can be written as

$$j_z = |e|(n_I w_I - n_e w_e) = |e|n_I(w + w_I) \quad (4)$$

This equation implies that the magnitude of the current is identical to that carried by the absolute velocity $(w + w_I)$ of the ions in space. Furthermore, the axial force may be written as

$$X_z/|e|n_I = w_I B/\psi_I \quad (5)$$

Hence, the axial force is directly proportional to the ion slip velocity in the direction of the applied electric field. The expression also indicates that the axial momentum is transferred directly to the ions from the electromagnetic field.

5) The relations expressed by the force ratio equation can be used to show that there is a wide range of values ψ_e and ψ_I for which the axial force per unit volume due to the induced Hall current is larger than the tangential force per unit volume generated by the applied current. The trends should be such that the particle atomic weight is large, the electron temperature is high, and the ionization level is either quite low or quite high. We note at this point that the axial force may be written in the following form:

$$X_z = -j_\theta B = \frac{\psi_e|B|j_z}{(1 + \psi_e\psi_I)}(1 - \Psi) \quad (6)$$

where

$$\Psi = |e|n_I w/j_z$$

The parameter Ψ turns out to have a controlling role in the region of operation and performance of the Hall current accelerator. Obviously, Ψ must be less than unity ($\Psi < 1$) for positive accelerating body forces to be given to the gas. Two alternate interpretations of Ψ will be given at this point.

First, we may write $\Psi = w/(w_I - w_e)$(w_e is negative). When the electrons are effectively trapped by the magnetic field, $\Psi = w/(w + w_I)$, where Ψ is the ratio of the mass velocity to the absolute ion velocity.

Second, if the velocity and ion density are fairly constant over the cross section, Ψ can be written in terms of parameters over which we have some control:

$$\Psi \equiv \frac{|e|n_I w}{j_z} \cong \frac{|e|\alpha nwA}{I}\cdot\frac{m_a}{m_a} = \frac{|e|\alpha\dot{m}}{m_a I} \equiv \bar{\Psi} \quad (7)$$

In the foregoing equation, we have used the degree of ionization $\alpha = n_I/n$ and the continuity equation $nm_a w = \dot{m}/A$, where $\dot{m}$ is the mass flow rate.

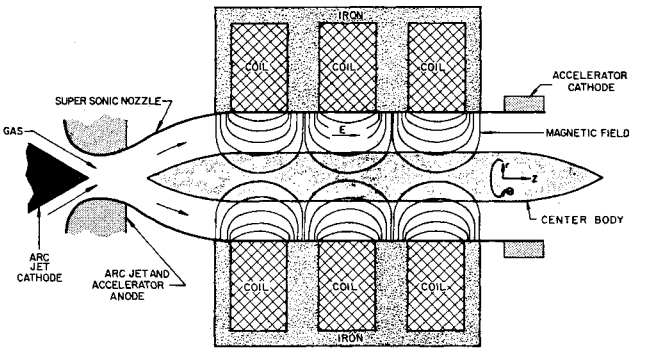

Fig. 1 Schematic diagram of a Hall accelerator.

2.2 Applied Electric Field Strength

A general expression for the electric field strength may be obtained from the tangential force equation:

$$E_z - vB = \frac{\psi_e w|B|}{(1 + \psi_e\psi_I)\Psi}\left\{\frac{(1 + \psi_I\psi_e)^2}{\Psi_e^2} + (1 - \Psi)\right\} \quad (8)$$

When the magnetic field is small, this expression reduces to

$$E_z = j_z/\sigma \quad \text{for} \quad \sigma \equiv |e|n_I\psi_e/|B| \quad (9)$$

However, as the magnetic field is increased, the electric field increases enough to cause appreciable ion slip so that a significant portion of the current is now carried by the ions.

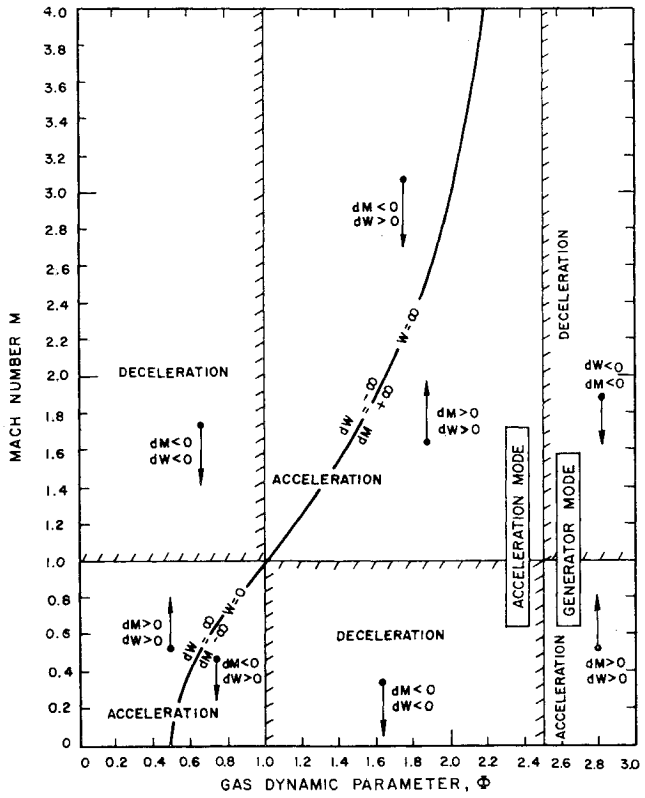

Fig. 2 Characteristic regions in M vs Φ plane.

In the strong magnetic field limit, when $\psi_e\psi_I \gg 1$, the electric field becomes

$$E_z - vB = (w|B|/\psi_I\Psi)\{\psi_I^2 + (1 - \Psi)\} \tag{10}$$

As long as the quantity Ψ is not close to unity, then an appreciable increase in the electric field results from the application of the radial magnetic field.

From Eq. (7), it may be seen that, if the gas remained in equilibrium and if it were possible to determine the gas temperature, then it would be possible to evaluate Ψ in terms of measured quantities and thus evaluate the value of $E - vB$, which is essentially the applied electric field as long as the tangential gas velocity remains small. What is perhaps more important is the fact that it should be possible to control the applied electric field strength by changing either the mass flow rate, the electric current, or the gas temperature.

3. Gasdynamics of the Hall Accelerator

In order to obtain some indication of the efficiency of conversion of electric power to effective jet power, a complete gasdynamic solution is necessary. The assumptions used to obtain the present solution to the Hall current accelerator are discussed below.

3.1 Assumptions and Equations Necessary to Obtain a Gasdynamic Solution

The effects of wall shear stress due to viscosity and of heat loss due to thermal conduction at the wall will be neglected. It also will be assumed that most of the gas mass flows through a constant area annulus in such a manner that gasdynamic properties can be averaged over the channel width. The equations of conservation of momentum and energy now become:

Conservation of Axial Momentum

$$\frac{d}{dz}(p + \rho w^2) = \frac{\psi_e|B|}{(1 + \psi_e\psi_I)}\frac{I}{A}(1 - \Psi) \tag{11}$$

where the right-hand side is obtained from the axial force equation derived previously.

Conservation of Tangential Momentum

$$(d/dz)(\rho w\, v) = IB/A \tag{12}$$

Conservation of Energy

$$\frac{d}{dz}\left\{\rho w\left(h + \frac{w^2}{2} + \frac{v^2}{2}\right)\right\} = \frac{w|B|\psi_e I}{\Psi(1 + \psi_e\psi_I)A}\left\{1 - \Psi + \left(\frac{1 + \psi_e\psi_I}{\psi_e}\right)^2 + \Psi\frac{v}{w}\frac{1 + \psi_e\psi_I}{\psi_e}\right\} \tag{13}$$

where the right-hand side is obtained using the applied electric field equation derived previously. Because of the initial assumptions, $\Psi = \bar{\Psi}$; furthermore, it can be argued[7] that the terms containing v are small compared to other terms. Hence, combining Eqs. (11) and (13), we now obtain

$$\frac{d}{dz}\left\{\rho w\left(h + \frac{w^2}{2}\right)\right\} = \frac{w}{\Psi}\left\{\frac{1 - \Psi + (1/\chi^2)}{1 - \Psi}\right\}\frac{d}{dz}(p + \rho w^2) \tag{14}$$

where

$$\chi \equiv \psi_e/(1 + \psi_e\psi_I)$$

We shall next assume that, over the length of the accelerator, the quantity

$$\frac{1}{\Psi}\left\{\frac{1 - \Psi + (1/\chi^2)}{1 - \Psi}\right\} \equiv \frac{\gamma}{\gamma - 1}\frac{1}{\Phi} \tag{15}$$

where Φ is a constant, and γ is the ratio of the specific heats for the gas. Equation (15) is completely justified for a fully ionized gas and for a partially ionized gas in which the percent ionization is constant throughout the accelerator length. The form of the assumption in Eq. (15) was chosen merely for convenience in reducing the equations. With the foregoing

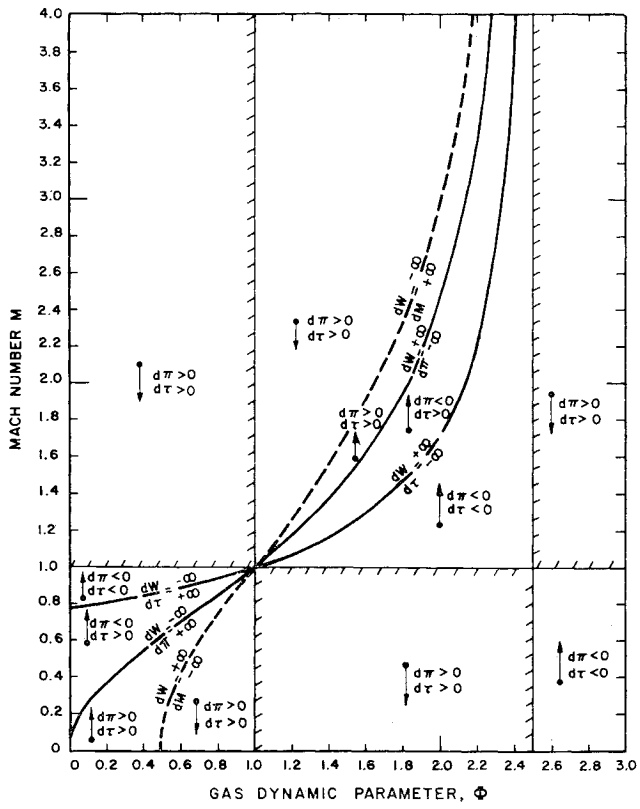

Fig. 3 Distinguished curves in the M vs Φ plane.

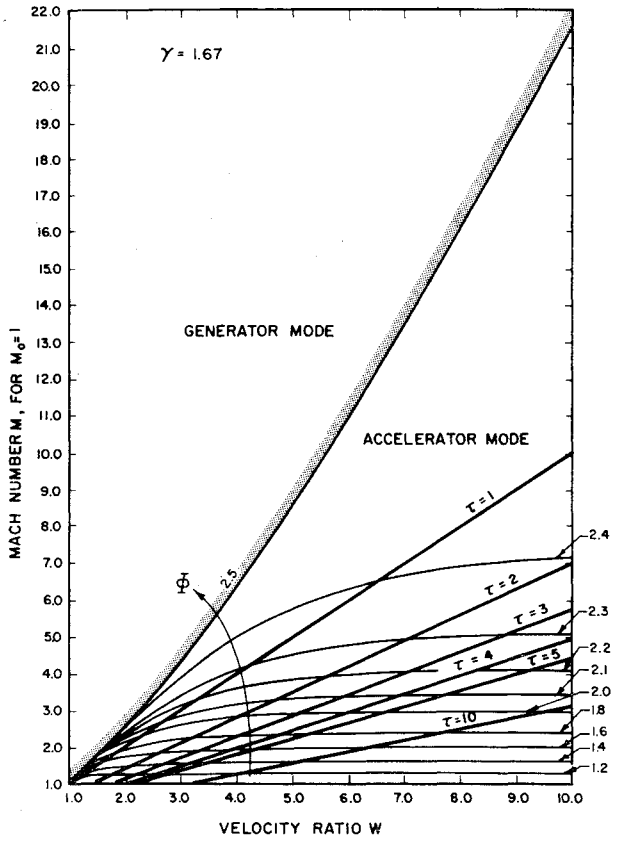

Fig. 4 Lines of constant Φ and τ in the M vs W plane.

assumptions, Eq. (14) can now be written in the following form (assuming a perfect gas):

$$d\left\{\rho w\left(\frac{\gamma}{\gamma-1}\frac{p}{\rho}+\frac{w^2}{2}\right)\right\}=\frac{\gamma}{\gamma-1}\frac{w}{\Phi}\,d(p+\rho w^2) \quad (16)$$

3.2 Differential Equations for the Hall Current Accelerator

A number of differential relations can be obtained from Eq. (16), the perfect gas relations, and the continuity equations which are useful in outlining the general performance characteristics of a Hall device. These are given below in terms of the parameters of Mach number M, specific heat ratio γ, and the quantity Φ.

Defining

$$W=\frac{w}{w_0} \qquad \pi=\frac{p}{p_0} \qquad \tau=\frac{T}{T_0} \quad (17)$$

where the zero subscripts refer to some initial values, we have

$$\frac{w}{p}\frac{dp}{dw}=\frac{\Phi(1-M^2)-\gamma M^2(1-\Phi)}{1-\Phi}=\frac{W}{\pi}\frac{d\pi}{dW} \quad (18)$$

$$\frac{w}{M}\frac{dM}{dw}=\frac{1}{2}\frac{2(1-\Phi)\{1+[(\gamma-1)/2]M^2\}-(1-M^2)}{1-\Phi}=\frac{W}{M}\frac{dM}{dW} \quad (19)$$

$$w\frac{dS/R}{dw}=\frac{\gamma}{\gamma-1}\left(1-\frac{\gamma-1}{\gamma}\Phi\right)\frac{1-M^2}{1-\Phi}=W\frac{dS/R}{dW} \quad (20)$$

$$M\frac{dS/R}{dM}=\frac{2\gamma}{\gamma-1}\frac{\{1-[(\gamma-1)/\gamma]\Phi\}(1-M^2)}{2(1-\Phi)\{1+[(\gamma-1)/2]M^2\}-(1-M^2)} \quad (21)$$

$$\frac{w}{T}\frac{dT}{dw}=\frac{(1-M^2)-(1-\Phi)(\gamma-1)M^2}{1-\Phi}=\frac{W}{\tau}\frac{d\tau}{dW} \quad (22)$$

Using Eqs. (19–21), it is possible to block out regimes in the plane of M vs Φ where various processes are occurring. (The entropy equations show the allowed direction of variation in W and M.) These are shown in Fig. 2. The limit line of velocity is obtained from the numerator of Eq. (19). The accelerator mode distinction may be applied when $\Psi < 1$. From Eq. (11), it may be seen that the body force is positive at this point and from Eq. (13) that the energy term is also positive. Of the six regimes outlined in the accelerator region, the one in which both Mach number and velocity increase during supersonic acceleration appears to be the most desirable. When operating in this region, a limiting Mach number is approached at the outlet, but the velocity can be made arbitrarily high. This is a very important result and indicates that there is no inherent upper limit to the velocity that is obtainable because of gasdynamic considerations. Viscous and heat conduction effects will modify this conclusion somewhat; hence, the Reynolds number is likely to be the significant parameter in determining the upper limit of velocity obtainable by a gas confined in an annular Hall accelerator.

In Fig. 3, curves are shown along which the temperature and pressure derivatives with respect to the velocity are zero. Between the Mach number 1 line and these curves, the temperature and pressure have been continually falling during the acceleration. Between these curves and the limit Mach number curve, the temperature and pressure rise.

3.3 Integral Relations for the Hall Accelerator

The differential relations shown by Eqs. (18–22) can be integrated, and the results are shown below:

$$\frac{M_0^2}{M^2}=1+\left\{1-\frac{\{1-[(\gamma-1)/\gamma]\Phi\}\gamma M_0^2}{2\Phi-1}\right\}\times\left\{\frac{1}{W^{(2\Phi-1)/(\Phi-1)}}-1\right\} \quad (23)$$

$$p/p_0=\pi=W(M_0^2/M^2) \quad (24)$$

$$T/T_0\equiv\tau=\pi W=W^2(M_0^2/M^2) \quad (25)$$

$$\Delta S/R=[\gamma/(\gamma-1)]\ln(\tau)-\ln(\pi) \quad (26)$$

These relations can be used to determine the over-all performance capability of the accelerator. A sampling of the computed performance data is shown in Figs. 4 and 5.

The values of constant temperature ratio plotted on Fig. 4 for $M_0 = 1$ helps to show that it is desirable to operate at fairly high values of the parameter Φ in order to keep the gas from heating excessively.

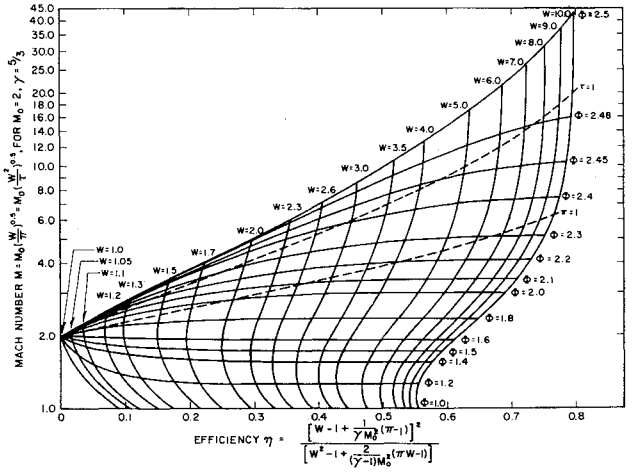

Fig. 5 Mach number as a function of efficiency, $M_0 = 2$, $\gamma = \frac{5}{3}$.

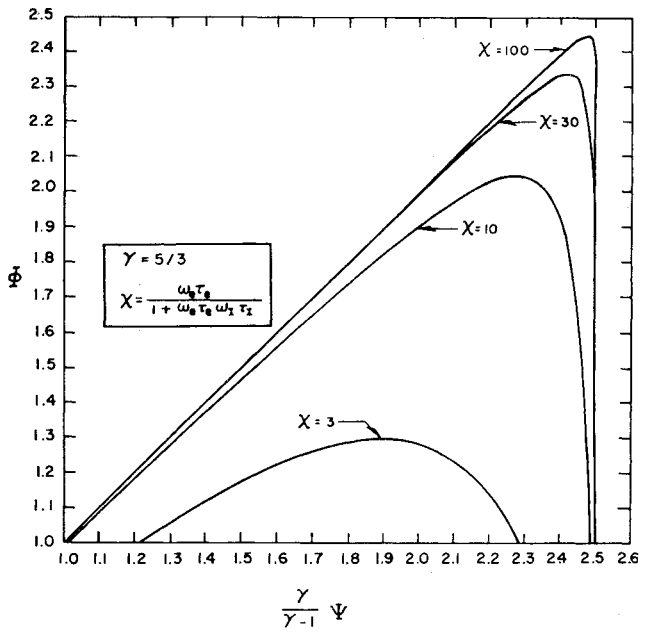

Fig. 6 Relation between gasdynamic parameter Φ and physical constant Ψ.

The thrust efficiency η is defined as follows:

$$\eta = \frac{\{A(p - p_0) + \dot{m}(w - w_0)\}^2}{2\dot{m}P} \tag{27}$$

where A is the cross-sectional area of the accelerator channel, P the electrical power input, and $\dot{m}$ the mass flow rate of the gas. The curves in Fig. 5 show the relation among the Mach number, the velocity ratio, and the efficiency when the initial Mach number has the value of 2 and the ratio of the specific heats for the gas is $\frac{5}{3}$.

3.4 The Relation between the Gasdynamic Variable Φ and the Flow Variable Ψ

The actual relation between these two quantities is shown in Eq. (15). The parameter

$$\psi_e/(1 + \psi_e\psi_I) = \chi$$

is determined from the average magnetic field strength and the gas properties $\psi_e/|B|$ and $\psi_I/|B|$. Equation (15) has been evaluated and is plotted over the accelerating region of interest in Fig. 6.

A very important result appears on this plot, namely, that there are two possible values of Ψ for each value of Φ and the parameter χ. In view of the form of Ψ, we shall call these two possible modes of operation the high-current and low-current modes. The former occurs for the lower value of Ψ and is probably the more desirable operating condition since, as will be seen in the next section, it can be done in a much shorter accelerator. Figure 6, in conjunction with Fig. 2, also shows that the exit Mach number attainable is reduced drastically as the parameter χ becomes less than 10. This fact is shown more clearly in Fig. 7, where the critical Mach curve is plotted as a function of the variable Ψ, with χ as a parameter.

3.5 Application of Analysis to the Design of a Hall Current Plasma Accelerator

The analytical work discussed below is an attempt to derive realistic design criteria from the general analysis presented in the previous sections. The study is carried out for argon gas only, since the Hall parameters for this gas have been evaluated previously. Expressions for the force per unit volume transmitted to the gas and the energy transferred to the gas as both work energy and internal energy are used to compute relations for the following quantities: 1) the effective velocity increment per centimeter of accelerator length, 2) the effective electrical conductivity of the gas, and 3) the local thrust efficiency defined as $[(\mathbf{J} \times \mathbf{B}\cdot\mathbf{U})/\mathbf{J}\cdot\mathbf{E}]$. Using these quantities, the design and operating parameters for a high-specific-impulse, high-efficiency engine can be determined.

3.5.1 *Effective velocity increment*

The expression for the force on the gas per unit volume can be rewritten as a net effective velocity increment per unit length which the gas acquires because of the interaction with the electromagnetic field. To obtain this velocity increment, integrate over the cross-sectional area and divide by the mass flow rate of the gas. The following expression is then obtained:

$$\Delta w_{\text{eff}} = \frac{|e|\alpha}{m_a}\chi B\frac{1 - \Psi}{\Psi} \times 10^{-2}\ \frac{\text{m}}{\text{sec-cm}} \tag{28}$$

Using the equilibrium properties of argon gas, it is possible to evaluate the foregoing expression as a function of the applied magnetic field strength and the parameter Ψ. It has been shown previously that Ψ must lie between 0.4 and 1.0 for supersonic acceleration. For convenience, the value of 0.70 for Ψ will be used in evaluating the effective velocity increment shown in the foregoing expression and in other expressions that follow in which Ψ appears.

A sample plot of effective velocity increment per centimeter of accelerator length as a function of the applied magnetic field strength is presented in Fig. 8. These curves exhibit the expected relation between the velocity increment and the magnetic field strength. The velocity increment rises initially with the magnetic field strength squared and then becomes asymptotically independent of the magnetic field strength.

When the gas is truly fully ionized, so that no atoms are present to allow ion diffusion or ion slip, then the velocity in-

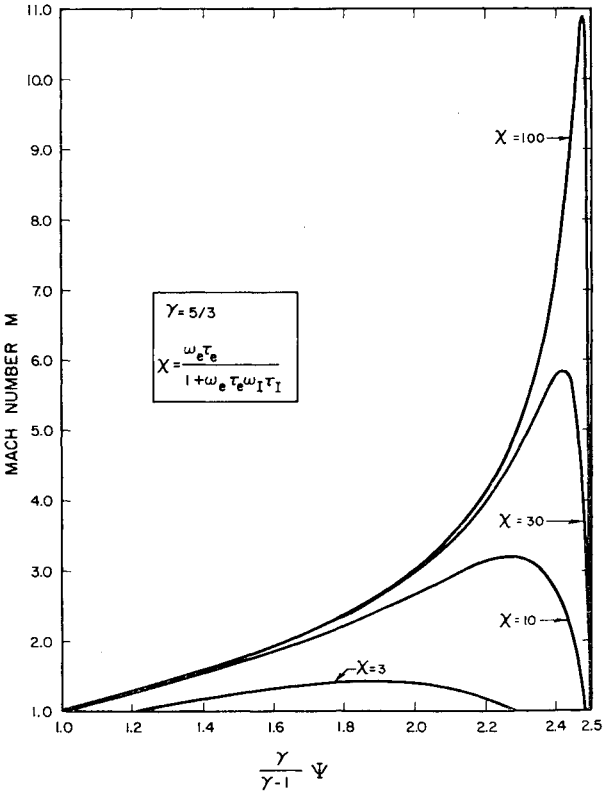

Fig. 7 Limit Mach number as a function of Ψ.

crement should always increase with the square of the magnetic field strength. In some cases of Fig. 8, the gas is ionized more than 98%. The few remaining atoms are, however, still adequate to allow sufficient ion slip so that the velocity increment becomes independent of the magnetic field strength.

3.5.2 *Effective electrical conductivity*

With $\sigma_z = j_z/E_z = \sigma_z(p, T, B_r)$, it is possible to write the following expression for the effective electrical conductivity:

$$\sigma_z = \frac{|e|}{m_a} \frac{\rho\alpha\chi B}{B^2 + (B\chi)^2(1 - \Psi)} \tag{29}$$

The dependence of σ_z on the magnetic field strength is complicated, but some regimes can be identified:

Regime 1

$$B^2 \gg (B\chi)^2(1 - \Psi) \qquad \psi_e\psi_I \ll 1 \tag{30}$$

σ_z is then equal to the scalar conductivity and independent of the magnetic field strength.

Regime 2

$$(B\chi)^2(1 - \Psi) > B^2 \qquad \psi_e\psi_I < 1 \tag{31}$$

In this regime the electron diffusion is impeded by the magnetic field, and the ions have not yet begun to have any appreciable slip. The magnitude of σ_z consequently drops with the square of the magnetic field strength.

Regime 3

$$(B\chi)^2(1 - \Psi) \gg B^2 \qquad \psi_e\psi_I > 1 \tag{32}$$

When the foregoing condition prevails, the electrons are effectively trapped by the magnetic field and the ions are conducting. The magnetic field is not yet affecting the ion diffusion rate, however, so that the actual magnitude of σ_z is independent of the magnetic field strength.

Regime 4

$$B^2 > (B\chi)^2(1 - \Psi) \qquad \psi_e\psi_I \gg 1 \tag{33}$$

The magnetic field has now become strong enough to impede the ion diffusion rate as well as that of the electrons. The value of σ_z now falls again with the square of the magnetic field strength.

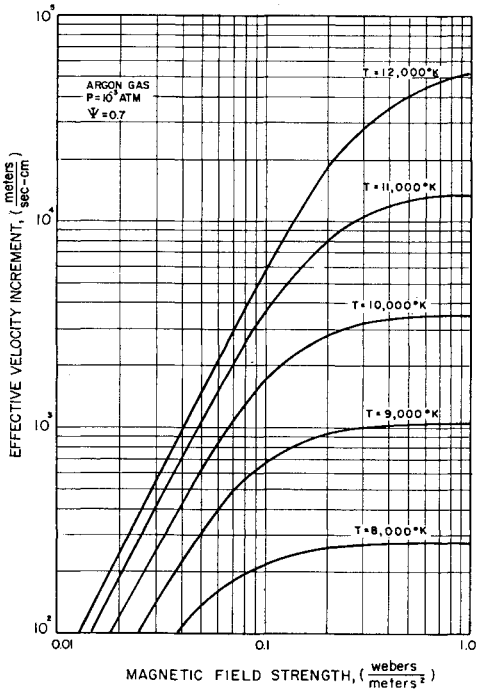

Fig. 8 Effective velocity increment per centimeter of accelerator length vs applied magnetic field strength; argon gas, $P = 10^{-3}$ atm.

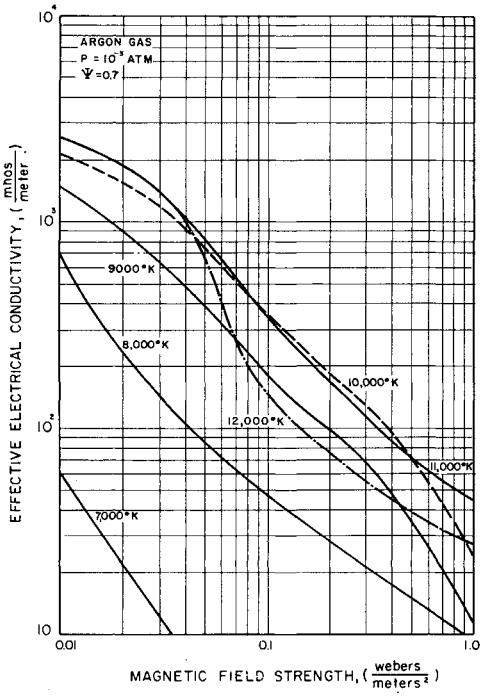

Fig. 9 Effective electrical conductivity as a function of the applied magnetic field strength; argon gas, $P = 10^{-3}$ atm.

The four regimes just outlined are not necessarily mutually exclusive. Hence, it may be possible for the value of σ_z to vary with the magnetic field in some relationship that falls between an inverse square law and a law indicating independence. For example, the effective conductivity may vary inversely as the linear power of the magnetic field strength, resulting in a linear dependence upon the magnetic field strength of the potential drop across the accelerator.

A sample plot of effective electrical conductivity is presented in Fig. 9 as a function of the magnetic field with the temperature as a parameter.

3.5.3 *Local efficiency*

When the tangential velocity component can be neglected compared to the axial velocity, the local thrust efficiency, $[(\mathbf{J} \times \mathbf{B}\cdot\mathbf{U})/\mathbf{J}\cdot\mathbf{E}]$, can be reduced to the following expression:

$$\eta_L = \Psi(1 - \Psi)/[(1/\chi^2) + 1 - \Psi] \tag{34}$$

A typical plot of the local efficiency is given in Fig. 10 as a function of the magnetic field strength with the gas temperature as a parameter. These curves indicate an interesting symmetry about an optimum magnetic field for each pressure if the accelerator operates over a temperature range. This occurs because of the form of the χ curves plotted against temperature.

3.5.4 *Summary and design parameters*

Using the data in the various plots of which only a sampling has been given here, criteria for the design of a high-performance Hall accelerator can be formulated and some assumptions made concerning viscous and thermal losses.

Probably the most important parameter that one should attempt to determine is the gas temperature in the accelerator. The quantities that will help to fix the operating temperature are the ionization level in the gas, the Mach number at the channel exit, and the interrelation among the Mach number, the parameters χ and Ψ, and the temperature. (This is partly exhibited in Fig. 7.) Since the speed of sound in argon is not high, being only about 2900 m/sec at 12,000°K, it

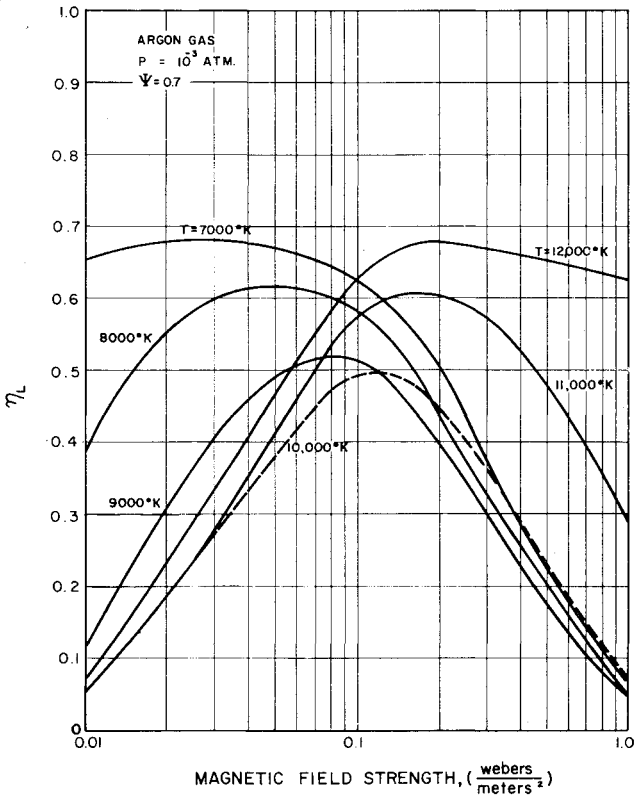

Fig. 10 Local efficiency for the Hall accelerator; argon gas, $P = 10^{-3}$ atm.

becomes evident that the exit Mach number of the gas must be high if exhaust velocities of over 20,000 m/sec are to be obtained. From Fig. 7, this implies that the accelerator must be operated in a temperature and pressure regime where the parameter χ is large and also where the quantity Ψ is only slightly less than unity. For the parameter χ to be greater than 10, the temperature must either be less than 6000°K or greater than 11,000°K. From the point of view of thermal and ionization energy losses, the low-temperature regime would appear to be the more desirable one in which to operate. However, the velocity increment attainable at gas temperatures of under 6000°K is, at most, 20 m/sec-cm. Because of viscous losses due to wall friction, this regime does not appear promising; hence, it seems essential to try to operate at gas temperatures of over 11,000°K. Over the pressure range from 10^{-4} to 10^{-2} atm, argon becomes practically fully singly ionized at temperatures of 11,000° to 12,000°K, and at higher temperatures, double ionization becomes significant. In order to keep the ionization loss to a minimum, the gas temperature, hence, should be kept lower than 15,000°K. The temperature of the gas in the accelerator therefore should be maintained between the limits of 11,000° and 15,000°K.

In the foregoing discussion, it was found desirable to operate the accelerator with Ψ only slightly less than unity so that the Mach number at the exit would be high. However, Eq. (33) indicates that the velocity increment per centimeter of accelerator length drops to zero as $\Psi \to 1$. It is obvious that some compromise must be made, and, for the time being, a value of $\Psi = 0.70$ is chosen as a reasonable value to design around, since Ψ must be between 0.40 and 1.0 for supersonic acceleration.

The static pressure at which the accelerator channel should be run can be found from plots of χ as a function of temperature, pressure, and magnetic field. In order to keep the value of the parameter χ of the order of 10 or greater, it turns out that the pressure must be between 10^{-3} and 10^{-4} atm. The magnetic field strength B can also be determined from these plots and from plots such as Fig. 10. These curves indicate that the ratio of the magnetic field strength to the static pressure should be kept constant at a value of about $B/p = 10^{-3}$ webers/newton. For pressures of 10^{-3} to 10^{-4} atm, the indicated radial magnetic field strength should be from 1000 to 100 gauss, respectively.

A set of design equations that will be useful in obtaining a first estimate of the characteristics of a high-performance Hall accelerator can now be written. We shall assume that the following information is given: 1) the total power input = arcjet power P_J + accelerator power P_A; 2) the required specific impulse or exit velocity w_{exit}; and 3) the conversion efficiency of electrical power into jet power η_1. The mass flow rate, current, accelerator length, and cross-sectional area can be determined from the following equations:

$$\dot{m} = \frac{2\eta_1(P_A + P_J)}{w^2_{exit}} \qquad I = \frac{|e|}{m_a}\frac{\dot{m}\alpha}{\Psi}$$
$$L = \frac{w_{exit}}{\Delta w_{eff}} \qquad A = \frac{I^2 L}{\sigma_z P_A} \tag{35}$$

In addition to the foregoing expressions, the equation for the conversion of mass must be satisfied. This expression can be used to calculate the static pressure at the exit of the accelerator as follows:

$$p_{exit} = \frac{(1+\alpha)\dot{m}RT_{exit}}{w_{exit}A} \tag{36}$$

The pressure calculated from this equation must be compatible with that chosen at the beginning or else the complete design must be re-evaluated until compatible values of the pressure are obtained.

For a sample calculation, we shall make the assumptions: $P = 200$ kw; P_J = arcjet power = 25 kw; P_A = accelerator power = 175 kw; $\eta_1 = 0.50$ = over-all efficiency; I_{sp} = 3000 sec; static pressure = 2×10^{-4} to 10^{-3} atm; average radial magnetic field = 200 to 1000 gauss; T = 11,000° to 12,000°K.

From these assumptions and the various plots, Δw_{eff} = 4000 to 5000 m/sec-cm, $\alpha = 1.0$, $\sigma_z = 200$ mho/m, $\dot{m}$ = 0.22 g/sec, $I = 765$ amp, L = 6 to 7.5 cm, A = 10 to 12.5 cm², and $p = 3.6 \times 10^{-4}$ atm.

4. Conclusions

The detailed mechanisms of energy and momentum exchange between the electromagnetic field and the ionized gas in a Hall current accelerator have been computed in very general terms. Physical interpretations of the mathematical expressions describing these processes have been carefully worked out.

Using the equations derived for the momentum and energy exchange in a Hall current accelerator, sample data for the performance of argon in an accelerator have been computed and presented in graphical form. These curves represent maximum performance capability, since all loss mechanisms, e.g., wall friction and heat transfer, were considered to be zero.

The gasdynamics of an idealized configuration for a Hall current accelerator have been worked out in detail. Sample performance curves for the device are presented which show the attainable thrust efficiencies and other important properties. It has been determined that an important parameter, $\Psi \equiv$ ratio of the ion flux density carried by the mean gas flow to the current density, characterizes Hall devices.

References

[1] Cann, G. L., Buhler, R. D., Teem, J. M., and Branson, L. K., "Magnetogasdynamic accelerator techniques," Final Rept., Contract AF 40(600)-939, Arnold Engineering Development Center (1961).

[2] Hess, R. V., Burlock, J., Sevier, J. R., and Brockman, P.,

"Theory and experiments for the role of space-charge in plasma acceleration," *1961 Proceedings of the Symposium on Electromagnetics and Fluid Dynamics of Gaseous Plasma* (Polytechnic Press, Brooklyn, N. Y., 1962).

[3] Sevier, J. R., Hess, R. V., and Brockman, P., "Coaxial current accelerator operation at forces and efficiencies comparable to conventional crossed-field accelerators," ARS J. **32**, 78–80 (1962).

[4] Powers, W. E. and Patrick, R. M., "Magnetic annular arc," Phys. Fluids **5**, 1196 (1962).

[5] Walch, A. P., Pinsley, E. A., and Davis, J. W., "Operating characteristics of the oscillating-electron ion engine," ARS Preprint 2451-62 (1962).

[6] Miller, D. B. and Gloersen, P., "Cyclotron resonance propulsion system," *Proceedings of the Third Symposium on the Engineering Aspects of Magnetohydrodynamics* (Columbia University Press, New York, 1962).

[7] Cann, G. L., Marlotte, G. L., and Ziemer, R. W., "A steady state Hall current accelerator," Final NASA Rept., Contract NAS3-2500, Lewis Research Center, Cleveland, Ohio (1963).

[8] Cann, G. L., "Energy transfer processes in a partially ionized gas," Memo. 61, Guggenheim Aeronautical Lab., California Institute of Technology (1961).

[9] Cann, G. L., "Transport properties of a three-component nonequilibrium plasma with application to MGD accelerators," ARS Preprint 2396-62 (1962).